Asian Journal of Mechanical Engineering
ISSN: 2249-6289 (P); 3049-1886 (E)
Vol.14 No.1, 2025, pp.18-31

www.crijournals.org
DOI: https://doi.org/10.70112/arme-2025.14.1.4286

Development of a Mathematical Model for Hypersonic Aircraft Scramjet Engine Dynamics

Zairil A. Zaludin
Department of Aerospace Engineering, University Putra Malaysia, Selangor, Malaysia
E-mail: zairil_azhar@upm.edu.my
(Received 23 January 2025; Revised 29 January 2025; Accepted 19 February 2025; Available online 8 March 2025)

***Abstract* - This study proposes a methodology to obtain several critical parameters of scramjet engine propulsion for a generic hypersonic aircraft mathematical model. Using available variables from the existing model, additional variables were computed in real time during simulations. The perturbation in the thrust force along the x-axis direction (ΔX_T) was applied as the fuel flow rate input to the mathematical model. Dynamic stability was maintained by the controlled aircraft, provided that the engine time constant did not exceed 0.07 s. The integration of the scramjet engine mathematical model within the generic hypersonic aircraft model exhibited a negligible effect on closed-loop stability.**
***Keywords*: Hypersonic Aircraft, Scramjet Engine, Fuel Flow Rate, Dynamic Stability, Mathematical Modelling**

I. INTRODUCTION

Air-breathing hypersonic aircraft may enable routine and cost-effective access to high-speed transportation. Research on such vehicles began in the 1960s and continued through the 1990s with the National Aerospace Plane (NASP) program. Despite decades of investigation, it is widely recognized that the development of a full-scale operational vehicle requires significant advancements in propulsion and materials technologies, as well as improvements in multidisciplinary modelling and design tools. Following the cancellation of the NASP in the early 1990s, research into scramjet-powered flight continued, albeit on a reduced scale. Several programs focused on demonstrating the feasibility of key component technologies necessary for sustained hypersonic flight. A notable example is NASA's successful flight tests of the scramjet-powered X-43A, a subscale technology demonstrator flown in 2004 and 2005. Additionally, the X-51 Scramjet Engine Demonstrator conducted its first flight in 2010.

The first comprehensive analytical model for the longitudinal dynamics of a hypersonic vehicle (HSV) was developed by Chavez and Schmidt [1]. Utilizing Newtonian impact theory, they derived analytical expressions for the pressure distribution on the vehicle. These pressures were influenced by parameters such as the Mach number, freestream pressure, angle of attack, and vehicle geometry. The expressions were further refined to obtain analytical representations of the total aerodynamic forces acting on the vehicle. The resulting equations were then linearized to yield analytical expressions for the stability and control derivatives. Ultimately, the requirements and control laws for the HSV were synthesized [1], [2]. The study of hypersonic aircraft flight dynamics based on these results was further advanced by McLean and Zaludin [3]. It was determined that the flaps on Hyperion-the name given to the hypersonic transport aircraft (HST) mathematical model-were the most active control surfaces in stabilizing longitudinal motion. However, as the aircraft's Mach number increased, the effectiveness of the flaps decreased. Moreover, using the flaps as the primary control mechanism at hypersonic speeds led to excessive aerodynamic heating, resulting in potential structural damage. Therefore, a better understanding of how the engine could be utilized more effectively was required. An extension of the same research was conducted to reconfigure the control law to maintain stability in the event of flap malfunction by relying on engine control [4]. This necessitated a deeper understanding of engine dynamics and their interaction with the airframe.

In the HST model, it became evident that Hyperion did not provide detailed engine modelling. The engine was assumed to be controlled through variations in diffuser area (ΔA_D) and combustor exit temperature (ΔT_o). By modifying A_D and T_o, the engine thrust could be indirectly adjusted; however, direct thrust control was not supported by the existing model. To better understand the implications of direct engine control on aircraft dynamics, it was proposed that ΔA_D and ΔT_o be used jointly to define a new control input, ΔT_h. The current engine dynamics model used in Hyperion required further development to accommodate this approach. As an initial step, a published mathematical model of engine dynamics for a similar hypersonic aircraft was adopted. The development of the enhanced engine dynamics model and its integration into Hyperion was based on the theoretical frameworks presented by Raney *et al.,* [5] and Chavez and Schmidt [1].

The contents of this article are organized as follows. Section II presents details of the proposed mathematical model of the engine dynamics for Hyperion. Section III describes the integration of the mathematical model of the engine dynamics into the controlled aircraft dynamics. The results of the test conducted on the engine dynamics are presented in Section IV. In Section V, the results of integrating the new engine dynamics with the aircraft dynamics are shown. In

that test, the aircraft was subjected to a commanded change in height. Inspection of the model's dynamic responses verified the integrity of the aircraft's stable closed-loop system with the proposed engine dynamics incorporated. The results of these studies showed that the mathematical model proposed for engine dynamics in Hyperion could be successfully developed using the simulation software package Simulink. Incorporating the engine dynamics into the controlled aircraft dynamics did not jeopardize the closed-loop dynamic stability of the aircraft, provided that the principal time constant associated with the engine dynamics did not exceed 0.07 s. The mathematical model of the engine dynamics provided engine information such as maximum specific impulse (I_{spmax}), specific impulse (Isp), fuel equivalence ratio (η), and net thrust (Th).

II. THE VEHICLE

For convenience of reference, the name HYPERION has been given to this mathematical model. A sketch of this hypothetical aircraft is shown in Fig. 1

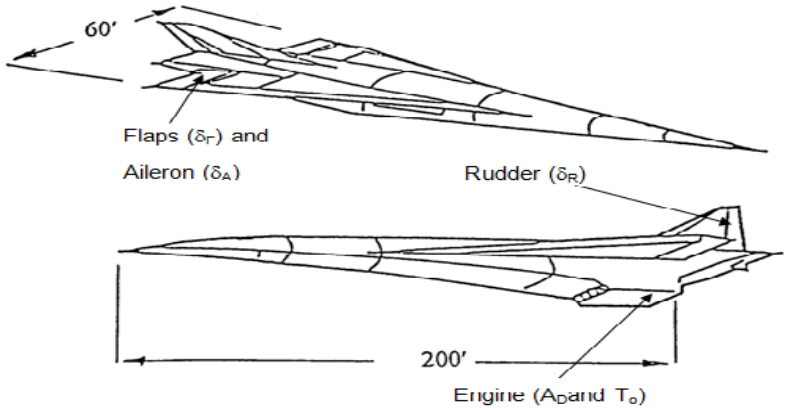

Fig. 1 The Generic Hypersonic Aircraft Sketch

The mathematical model was linear and had five control inputs, viz.:

- δ_F denotes flap surface deflection.
- A_D denotes the ratio of engine diffuser area.
- T_o denotes the temperature across the engine combustor.
- δ_A denotes aileron deflection.
- δ_R denotes rudder deflection.

The first three controls were used for controlling longitudinal motion, and the final two were used for controlling the aircraft's lateral motion. The Hyperion concept was based on the work by Chavez and Schmidt [1]. These authors conducted a thorough analysis of the mathematical model of the hypersonic aircraft on a two-dimensional representation, which is shown as Fig. 2.

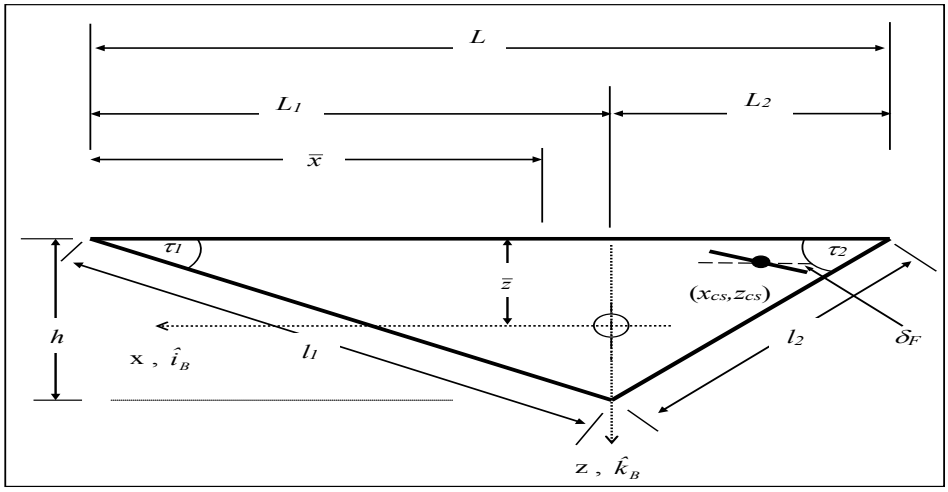

Fig. 2 Two-Dimensional Representation and Geometrical Details of the HST Vehicle

By using this two-dimensional model, two important features simplified the analysis of the dynamic characteristics of the aircraft: a forebody compression surface and an afterbody/nozzle expansion surface. The lower forebody compression surface served as a lifting surface and acted as an external diffuser for the engine. The vehicle's afterbody and nozzle surfaces functioned as external expansion nozzles, producing both thrust and lift. Table I presents the aircraft geometry data used for all the mathematical models of longitudinal motion considered in this paper.

TABLE I AIRCRAFT GEOMETRY DATA

AIRCRAFT GEOMETRY			
τ_1	=0.24435 rad (14°)	δ_O	=0.52395 rad (30.02°)
τ_2	=0.34907 rad (20°)	h	=22.20 ft
L	=150 ft	$\Delta\tau_1$	=1.7453×10^{-2} rad (1°)
L_1	=89.02ft	$\Delta\tau_2$	=1.7453×10^{-2} rad (1°)
L_2	=60.98 ft	m	=500 slug/ft
$\frac{S_{cs}}{b}$	=22.5ft	m	=40 slug/ft
$\bar{x}$	=90.00 ft	g	=32.2 ft/s^2
$\bar{z}$	=11.25 ft	I_{yy}	=1.0×10^6 slug ft^2/ft
x_{cs}	=-52.50 ft	ω_1	=18 rad/s
z_{cs}	=-11.25 ft	ζ_1	=0.02
l_1	=91.756 ft	l_2	=64.894 ft

I_{yy} is the inertia per unit width about the Y-axis, S_{cs} is the control surface reference area, ω_1 is the frequency of the first in-vacuo vibration mode, $\zeta_1$is the damping ratio of the first in-vacuo vibration mode, m is the vehicle mass per unit width, and m is the generalised elastic mass per unit width.

III. THE PROPOSED MATHEMATICAL MODEL OF THE ENGINE DYNAMICS

The mathematical model of the engine dynamics was constructed using a dynamic system simulation software, Simulink. The constructed model (Langley Visual/Motion Simulator (VMS) Hypersonic Propulsion Model) was based on the engine dynamic work published by Raney *et al.,*[5] and Raney and Lallman [6].

The fuel flow rate, w_f, was the command input for the proposed engine dynamics. For this work, it was assumed that the aircraft's Mach number and altitude were constant. The commanded fuel flow rate was used together with the aircraft Mach number and the dynamic pressure to compute a fuel equivalence ratio, η, which was used in association with an interpolation table to compute the specific impulse, I_{sp}. The relationship was valid for η ≤ 1. A penalty was applied for η > 1 in the form of an upper limit on specific impulse. In an air-breathing engine, specific impulse is a measure of fuel efficiency. For hypersonic propulsion systems, the best efficiency occurs at a fuel equivalence ratio of 1. As this ratio is adjusted above 1, the fuel efficiency drops off, and specific impulse decreases. A correction factor is applied in the form of limiting the specific impulse to reflect this decrease in efficiency. The product of I_{sp} and w_f determined the net thrust, *Th*. It is worth noting that the engine model used by Raney and Lallman [6] did not account for propulsion sensitivities to variations in angle of attack and body angular rates. The procedure for calculating η, I_{sp} and *Th* is shown in the next section. For the proposed engine dynamics, the net thrust is assumed to act only along the aircraft OX-axis. See Fig. 2.

A. Fuel Flow Rate, w_f

The fuel flow rate, w_f, depended upon the fuel flow rate command, w_{fcomm}. w_f was calculated from the equation below.

$$w_f = \frac{w_{fcomm}}{1+Ts} \quad (1)$$

where *T* represents the engine time constant. For this work, the engine time constant was taken to be 0.5s.

B. A Function of Mach Number, $f_1(M)$

The function $f_1(M)$ as shown in Fig. 3 depended upon the natural log of Mach number (*M*)

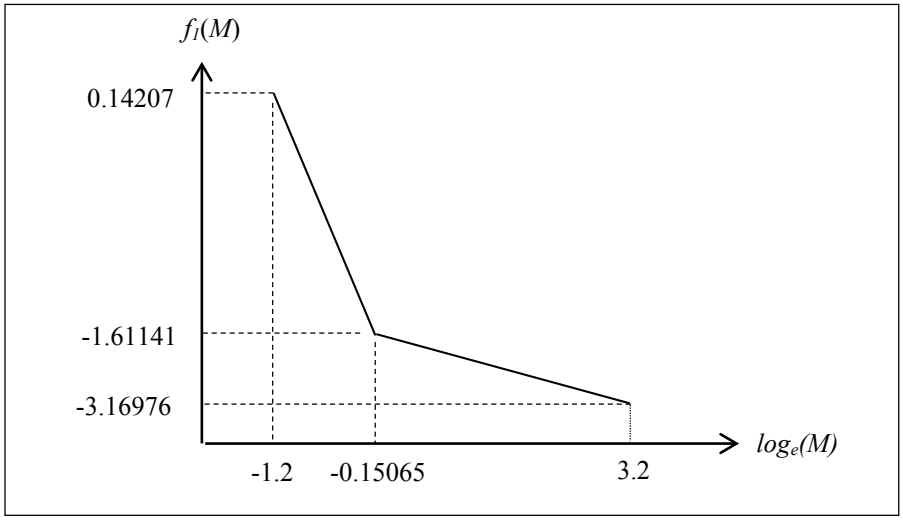

Fig. 3 A Function of Mach Number

C. The Ideal Flow Rate, $\boldsymbol{w_f}\big|_{\boldsymbol{\eta=1}}$

The ideal flow rate was the fuel flow rate when the fuel equivalence ratio was equal to unity. $w_f\big|_{\eta=1}$ was found from Eqn (2) i.e.

$$w_f\big|_{\eta=1} = q_\infty e^{f_1(M)} \tag{2}$$

where q_∞ represents the dynamic pressure.

D. The Fuel Equivalence Ratio, η

The fuel equivalence ratio was to be found using Eqn (3) viz.

$$\eta = \frac{w_f}{w_f\big|_{\eta=1}} \tag{3}$$

E. Specific Impulse Function with Unity Fuel Equivalence Ratio, $\hat{I}_{sp}$

The specific impulse for η = 1 at a specific Mach number was obtained from Fig. 4.

F. The Specific Impulse Function when Fuel Equivalence Ratio is Not Unity

To determine the limit on the specific impulse when η ≠ 1, a second non-linear specific impulse function was required. The graph of this function can be seen in Fig. 5.

G. Maximum Specific Impulse, I_{spmax}

The maximum specific impulse was found using Eqn (4).

$$I_{spmax} = \frac{f_2(M)}{\eta} \tag{4}$$

H. Net Thrust, Th

Finally, the net thrust for the engine dynamics was calculated using Eqn (5).

$$Th = I_{sp} w_f \tag{5}$$

IV. METHODOLOGY TO INTEGRATE THE ENGINE DYNAMICS WITH THE CONTROLLED AIRCRAFT DYNAMICS

The primary input for the engine dynamics is the fuel flow rate command, , w_{fcomm}, which must be obtained from the mathematical model of the aircraft dynamics. However, such a command variable was not directly available in the model proposed by Chavez and Schmidt [1], upon which Hyperion was based. Therefore, it was proposed that , w_{fcomm}, be represented as the perturbation in the thrust force, (ΔX_T), expressed in terms of the stability and control derivatives related to thrust.

This information was obtained from Chavez and Schmidt [1] and subsequently computed using Simulink. For convenience, the equation used to obtain (ΔX_T) is reproduced below.

$$\begin{Bmatrix} \Delta X_T \\ \Delta Z_T \\ \Delta M_T \\ \Delta Q_T \end{Bmatrix} = [T] \begin{Bmatrix} \Delta M_\infty \\ \Delta\alpha \\ \Delta q \\ \Delta\eta \\ \Delta\dot{\eta} \end{Bmatrix} + [T_c] \begin{Bmatrix} \Delta A_D \\ \Delta T_o \end{Bmatrix} \tag{6}$$

where

$$[T] = \begin{bmatrix} (X_T)_{M_\infty} & (X_T)_\alpha & (X_T)_q & (X_T)_\eta & (X_T)_{\dot{\eta}} \\ 0 & 0 & 0 & 0 & 0 \\ (M_T)_{M_\infty} & (M_T)_\alpha & (M_T)_q & (M_T)_\eta & (M_T)_{\dot{\eta}} \\ 0 & 0 & 0 & 0 & 0 \end{bmatrix} \tag{7}$$

$$[T_c] = \begin{bmatrix} (X_T)_{A_D} & (X_T)_{T_o} \\ 0 & 0 \\ (M_T)_{A_D} & (M_T)_{T_o} \\ 0 & 0 \end{bmatrix} \quad (8)$$

To find ΔX_T only, Eqn (6) was re-written using Eqn (7) and (8) as shown in Eqn (9).

$$\{\Delta X_T\} = [T_x] \begin{Bmatrix} \Delta M_\infty \\ \Delta\alpha \\ \Delta q \\ \Delta\eta \\ \Delta\dot{\eta} \end{Bmatrix} + [T_{\text{cx}}] \begin{Bmatrix} \Delta A_D \\ \Delta T_o \end{Bmatrix} \quad (9)$$

where

$$T_x = [(X_T)_{M_\infty} \quad (X_T)_\alpha \quad (X_T)_q \quad (X_T)_\eta \quad (X_T)_{\dot{\eta}}] \quad (10)$$

and

$$T_{\text{cx}} = [(X_T)_{A_D} \quad (X_T)_{T_o}] \quad (11)$$

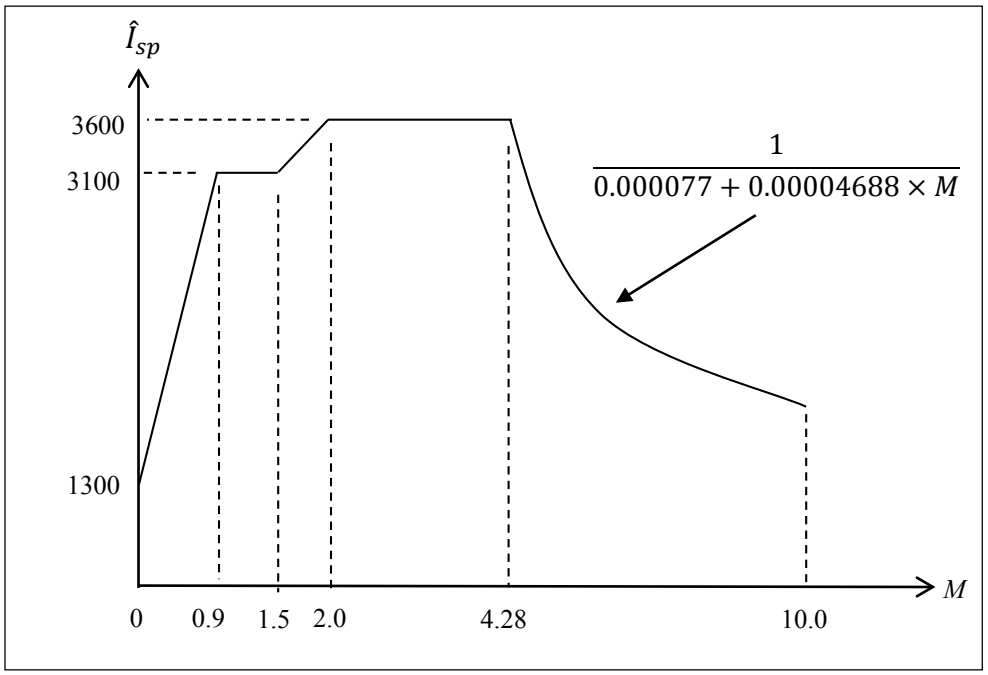

Fig. 4 Specific Impulse Function when Fuel Equivalence Ratio = 1

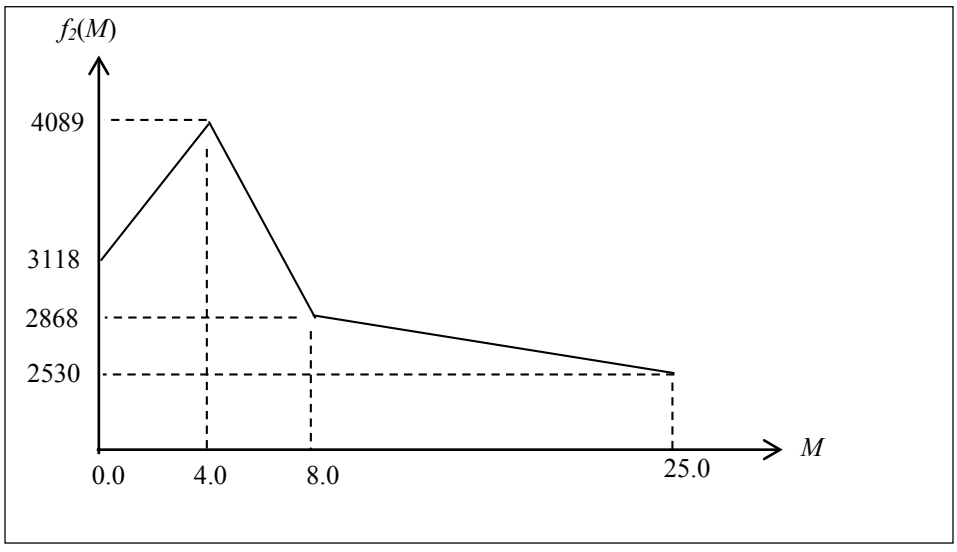

Fig. 5 Specific Impulse Function Limit As A Function Of Mach Number When Fuel Equivalence Ratio ≠ 1

Using ΔX_T as the fuel flow rate command, w_{fcomm}, the net thrust, *Th*, produced by the engine dynamics was found by using the Simulink model built earlier. To integrate the proposed engine dynamics with the aircraft dynamics required that *Th* be decomposed back into separate control variables, ΔA_D and ΔT_o. To do this, Eqn (9) was manipulated

in such a way that ΔA_D and ΔT_o could be recovered. The equation required to find ΔA_D and ΔT_o was Eqn (12).

$$\begin{Bmatrix} \Delta A_D \\ \Delta T_o \end{Bmatrix} = [T_{\text{cx}}]^{+} \left\{ [\Delta X_T] - [T_x] \begin{bmatrix} \Delta M_\infty \\ \Delta\alpha \\ \Delta q \\ \Delta\eta \\ \Delta\dot{\eta} \end{bmatrix} \right\}$$

where $[\ ]^{+}$ denotes a pseudo-inverse matrix.

Note that the Moore-Penrose pseudoinverse of the matrix T_{cx} was used to obtain ΔA_D and ΔT_o because the matrix T_{cx} is not a square matrix. All the pseudoinverse operations involved in this work were obtained using MATLAB. However, inverting T_{cx} using the pseudoinverse technique did not mean that a complete decomposition of the vectors ΔA_D and ΔT_o was always possible. This is because the pseudoinverse matrix of a rectangular matrix does not have all the properties of an inverted non-singular square matrix. If the recovered control input vectors ΔA_D and ΔT_o were not identical to the original variables, there was a strong possibility that the aircraft's closed-loop dynamic stability might be lost.

V. RESULTS FROM TESTING NEW ENGINE DYNAMICS

An experiment was conducted to test the mathematical model of the engine dynamics from Raney *et al.,*[4]. Using Simulink, the mathematical model was simulated for the aircraft operating at various Mach numbers. Consequently, the associated dynamic pressure varied. The simulations were performed for the aircraft flying at an altitude of 85,000 ft. Selected results obtained from the Simulink model are presented and discussed below.

A. Fuel Flow Rate vs. Time

The mathematical model was simulated for the aircraft flying at Mach 8.0 and an altitude of 85,000 ft, corresponding to a dynamic pressure, , q_∞, of 2082.5 lb/ft^2. The commanded fuel flow rates used were 100 lb/s, 200 lb/s, and 500 lb/s. The engine time constant was chosen to be 0.5 s. The fuel flow rate responses with respect to time are shown in Fig. 6.

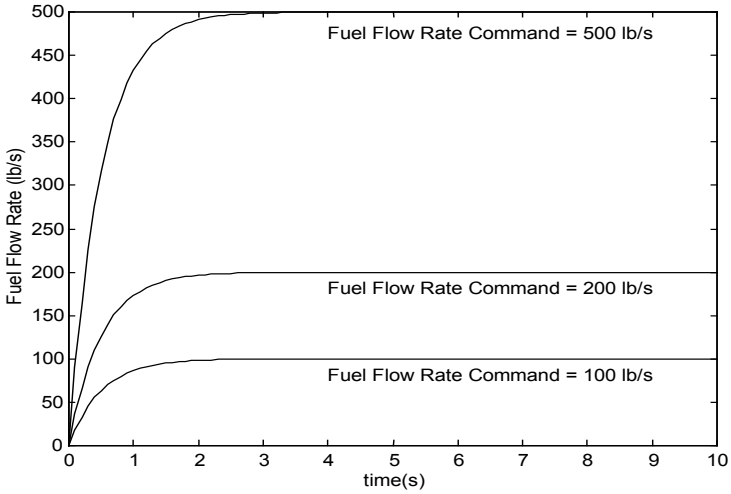

Fig. 6 The Fuel Flow Rate Dynamic Responses With Time

The dynamics of the fuel flow rate exhibited responses consistent with the engine time constant. At t=0.5 s, the dynamic response of the fuel flow rate to a command of 100 lb/s was 63.2 lb/s, which is 63.2% of the steady-state value. At t=2.5 s, the flow rate response reached the steady-state value of 100 lb/s. Similar responses were observed for the other commanded fuel flow rates.

B. The Mach Number Function

The graph in Fig. 3 was evaluated next using the Simulink model. Various Mach numbers were applied, while the mathematical model of the engine dynamics was assumed to correspond to the HST flying at an altitude of 85,000 ft. The results obtained are presented in Table II, and they correspond well with the graph in Fig. 3.

C. The Specific Impulse Function with Unity Fuel Equivalence Ratio

Using the same range of Mach numbers, the Simulink block for the specific impulse function, $\hat{I}_{SP}$ was tested. The results obtained are presented in TABLE III.

From Fig. 4, the specific impulse values, $\hat{I}_{SP}$, for the same Mach numbers were checked using the equation for the curve, viz.

$$\hat{I}_{SP} = \frac{1}{0.000077 + 0.00004688 \times M} \tag{13}$$

The $\hat{I}_{SP}$ obtained using the Simulink model corresponded with the results obtained using Eqn (13).

D. The Specific Impulse Function for Non-Unity Fuel Equivalence Ratio

Using the same set of Mach numbers, the Simulink block for the specific impulse function when the fuel equivalence ratio was not unity was tested. The values of $f_2(M)$ obtained from the Simulink model were found to be consistent with the values plotted in Fig. 5. The results obtained are presented in table IV.

TABLE II RESULTS FROM INTERPOLATING THE MACH NUMBER FUNCTION

Mach Number (M)	**Dynamic Pressure (lb/ft^2)**	$log_e(M)$	$f_1(M)$
8.0	2082.5	2.0794	-2.649
9.0	2635.7	2.1972	-2.703
10.0	3253.9	2.3026	-2.752
12.0	4685.7	2.4849	-2.837
15.0	7321.4	2.7081	-2.941

TABLE III THE SPECIFIC IMPULSE VALUES FOR FUEL EQUIVALENCE RATIO OF UNITY AT VARIOUS MACH NUMBERS.

Mach Number (M)	$\hat{I}_{SP}$
8.0	2212
9.0	2004
10.0	1832
12.0	1564
15.0	1282

TABLE IV THE SPECIFIC IMPULSE VALUES FOR NON-UNITY FUEL EQUIVALENCE RATIO AT VARIOUS MACH NUMBERS.

Mach Number (M)	$f_2(M)$
8.0	2868
9.0	2848
10.0	2828
12.0	2788
15.0	2729

TABLE V OTHER RESULTS OBTAINED FROM THE ENGINE DYNAMICS MATHEMATICAL MODEL.

Mach Number	$w_f\big\vert_{\eta=1}$ **(lb/s)**	η	I_{spmax} **(sec)**	$\hat{I}_{SP}$ **(sec)**	Th **(lb)**
8.0	147.3	0.6787	4226	2212	2.212×10^5
9.0	176.5	0.5665	5028	2004	2.004×10^5
10.0	207.5	0.4819	5069	1832	1.832×10^5
12.0	274.5	0.3642	7655	1564	1.564×10^5
15.0	386.7	0.2586	10550	1282	1.282×10^5

The values obtained from the Simulink model of the engine dynamics for the ideal fuel flow rate, fuel equivalence ratio, maximum specific impulse, specific impulse, and net thrust at different Mach numbers are presented in Table V. For all tests, a fuel flow rate command of 100 lb/s was applied.

It is noted that the net thrust of the engine dynamics decreases with increasing Mach number due to the reduction in specific impulse. The responses of the fuel equivalence ratio and thrust with time at various Mach numbers are shown in Fig. 7 and Fig. 8.

The results from this experiment demonstrate that the mathematical model of the engine dynamics, constructed using Simulink, produced outputs consistent with the formulae and graphs presented in the preceding sections.

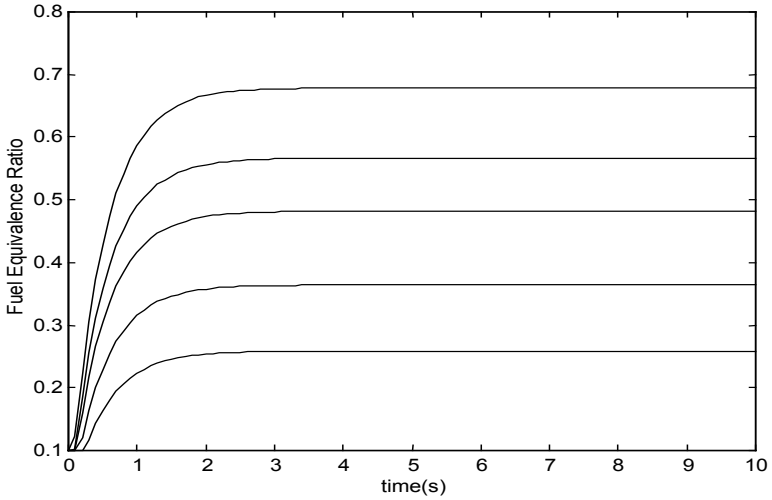

Fig. 7 The Response Of The Fuel Equivalence Ratio With Time.

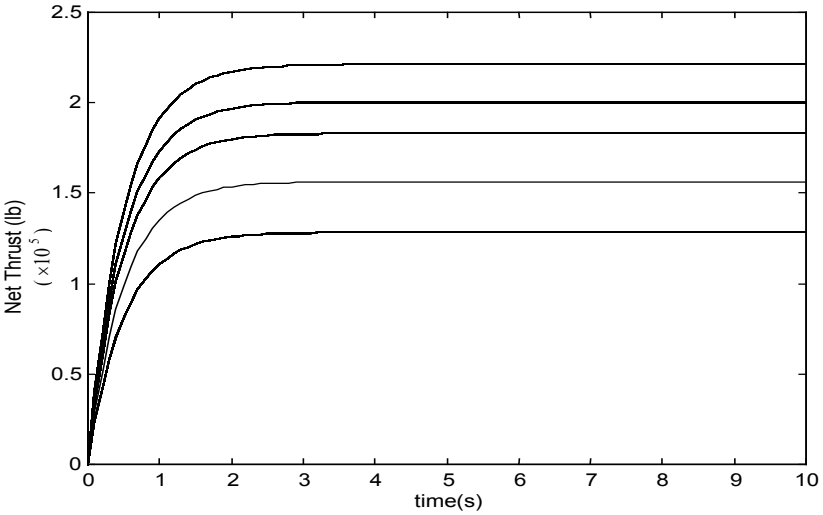

Fig. 8 The Response of Thrust with Time Atvarious Mach Numbers

VI. INCORPORATING THE ENGINE DYNAMICS MATHEMATICAL MODEL INTO THE CONTROLLED HYPERSONIC AIRCRAFT DYNAMICS

In [2], Hyperion flying at Mach 8.0 and an altitude of 85,000 ft without a Stability Augmentation System (SAS) was shown to be dynamically unstable. Subsequently, an SAS was designed for Hyperion using Linear Quadratic Regulator (LQR) theory. With the SAS, Hyperion's aircraft dynamics were stabilized. As indicated earlier in this paper, loss of closed-loop stability may occur when incorporating the proposed engine dynamics into Hyperion's closed-loop system using the proposed technique. In this section, Hyperion flying at Mach 8.0 and an altitude of 100,000 ft was used to test the closed-loop stability with the engine dynamics included.

Hyperion's closed-loop system without the engine dynamics is represented by the block diagram in Fig. 9. Hyperion flying at Mach 8.0 and an altitude of 100,000 ft was dynamically unstable [7]. Therefore, an SAS was required to stabilize the aircraft.

The results and responses obtained from the controlled Hyperion are compared with those obtained from the mathematical model used by Chavez and Schmidt [1]. Both models correspond to the HST aircraft flying at Mach 8.0 and an altitude of 100,000 ft, but inspection of the coefficient matrices A and B revealed that they were not identical. Consequently, it was expected that the responses from the two aircraft would differ. However, as discussed in [4], a method exists by which a controller can be designed for any aircraft such that the controlled aircraft exhibits natural modes specified by the designer. To make the comparison more meaningful, it was decided that, under control, both Hyperion and the mathematical model used by Chavez and Schmidt [1] should display the same natural modes. Ensuring that both aircraft have identical closed-loop eigenvalues satisfies (14).

$$\text{eig}\,[A_{LONG100K} - B_{LONG100K} \times K_{HYP}] = \text{eig}\,[A_{CS} - B_{CS} \times K_{CS}] \quad \text{- (14)}$$

The left-hand side of Eqn (14) represents the eigenvalues of the closed-loop dynamics of Hyperion, and the right-hand side represents the eigenvalues of the closed-loop dynamics of the mathematical model used by Chavez and Schmidt [1].

$$Q = \text{diag}\begin{bmatrix} 0.053 & -1.5358 \times 10^{6} & 1649.1 & 3.4755 \times 10^{6} & \dots \\ & & \dots & -1.05 \times 10^{-5} & 2.55 \times 10^{5} \quad 204.5 \end{bmatrix} \quad (15)$$

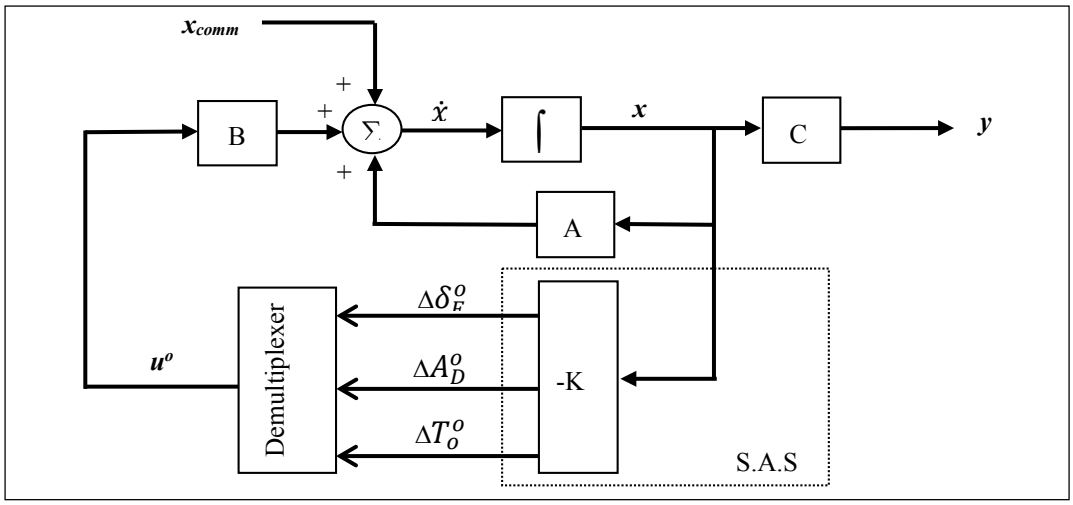

Fig. 9 Hyperion with a S.A.S flying at Mach 8.0 and at a height of 100000ft.

For Hyperion, the state-weighting matrix required to achieve those closed-loop eigenvalues as specified in table VI was derived using the control-weighting matrix Eqn (16) and the method discussed in [4]. The state-weighting matrix that resulted can be seen as Eqn (15).

$$G = \begin{bmatrix} 1 & 0 & 0 \\ 0 & 1 & 0 \\ 0 & 0 & 1 \end{bmatrix} \quad (16)$$

TABLE VI THE CHOSEN CLOSED-LOOP EIGENVALUES

Desired Closed-Loop Eigenvalues
$\sigma_{1,2} = -5 \pm j18$
$\sigma_{3,4} = -40 \pm j12$
$\sigma_{5,6} = -0.04 \pm j0.012$
$\sigma_{7} = -10$

When these weighting matrices were used to minimise the LQR performance index, the feedback gain matrix that resulted is shown in Eqn (17).

$$K^T = \begin{bmatrix} 0.026 & -0.237 & -0.0001 \\ 391.07 & -336.9 & -1.63 \\ -63.47 & -4.79 & 0.0166 \\ -1694.8 & -157.03 & 1.67 \\ 0.00074 & 0.0016 & 2.3 \times 10^{-6} \\ 96.45 & -285.9 & 0.017 \\ 5.89 & -14.0 & 0.0001 \end{bmatrix}$$

The closed-loop eigenvalues were found to be identical to those specified in table VI. The closed-loop aircraft control system responses to a commanded change in height of 1000ft are simulated in Fig. 10.

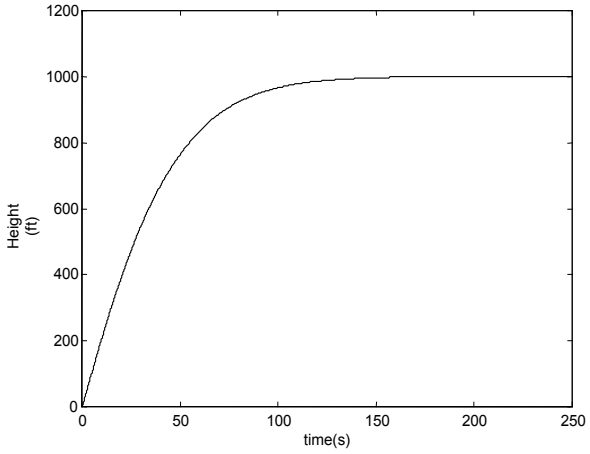

Fig. 10 Height response to a commanded change in height of 1000ft.

It can be observed from these responses that the controlled aircraft was stable. The altitude response reached a steady-state value of 1000 ft after 225 s. No phugoid or short-period mode was detectable in the Δα and Δθ responses, as shown in Fig. 11. The Δα response reached a steady-state value of 0.00397 rad (0.2°) after 200 s, and Δθ settled at 0.00136 rad These responses indicate that α and θ were minimally perturbed by the commanded change in altitude.

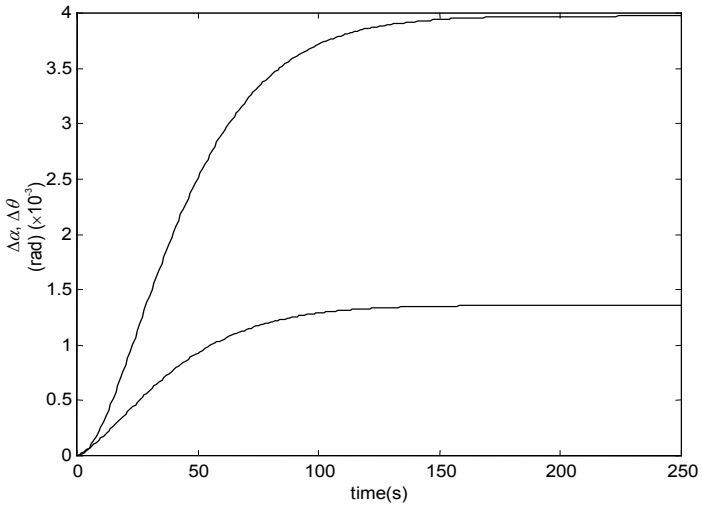

Fig. 11 Angle of attack and pitch attitude responses to a commanded change in height of 1000ft

Using the same mathematical model of Hyperion flying at Mach 8.0 and an altitude of 100,000 ft with the SAS, the proposed engine dynamics were incorporated into the aircraft dynamics. The intention was to integrate the proposed engine dynamics into Hyperion with the previously designed SAS. Fig. 12 illustrates the position of the engine dynamics within the aircraft dynamics block diagram.

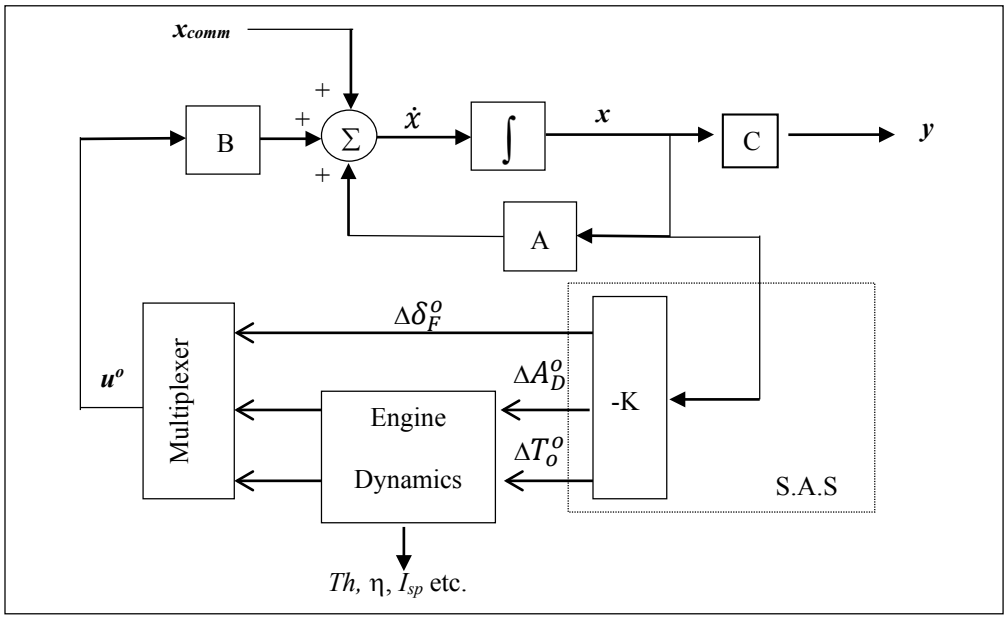

Fig. 12 Hyperion with the proposed engine dynamics

The aircraft responses to a commanded altitude change of 1000 ft were simulated again. The inputs for the engine dynamics were the fuel flow rate, assuming constant Mach number and dynamic pressure. The Mach number was 8.0, and the dynamic pressure was 1049.1 lb/ft². Note that ΔX_T was used as the commanded fuel flow rate (w_fcomm), since no direct information on the fuel flow rate was available from the aircraft dynamics. To obtain ΔX_T, the simulation software package Simulink was employed. Equation (9) can be represented by the block diagram in Fig. 13. With ΔX_T acting as w_{fcomm} in the block diagram, the engine net thrust, *Th*, was determined. After obtaining the net thrust, it had to be conditioned before reintroducing it into the aircraft dynamics. *Th* then had to be re-converted back to ΔX_T. The difficulty, however, was that a first-order transfer function existed relating w_f and w_{fcomm}. Inverting such a transfer function is not straightforward. No attempt was made in this work to perform the inversion. Instead, *Th* was divided by I_{SP} (see (5)) to obtain w_f, which was used instead of w_{fcomm} as the reconstructed ΔX_T (denoted by ΔX_{TR} from this point on). Using Eqn (12), the reconstructed engine controls, ΔA_{DR}^o and ΔT_{oR}^o, were then obtained. The construction of ΔX_{TR}, ΔA_{DR}^o and ΔT_{oR}^o is shown below in the block diagram of Fig. 14.

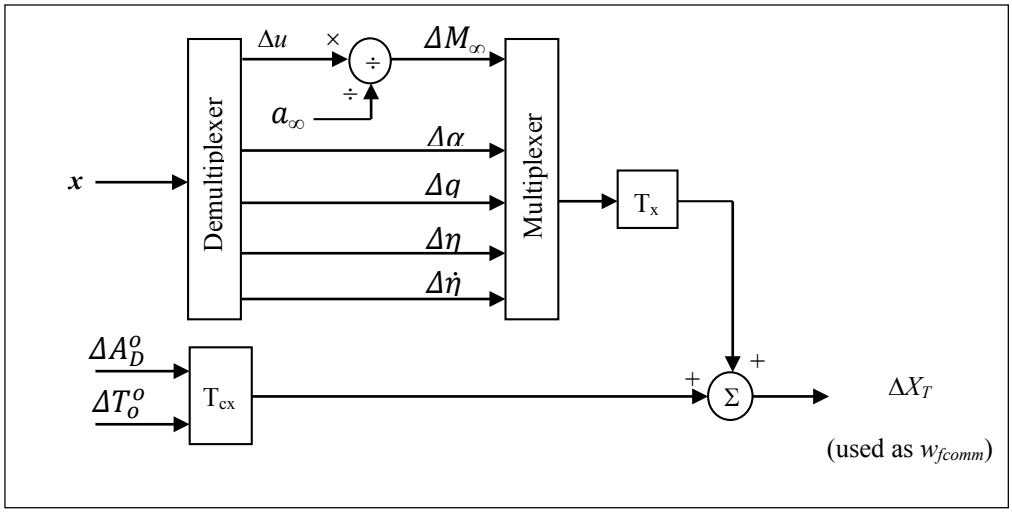

Fig. 13 Eqn (9) In Block Diagram To Derive ΔX_T

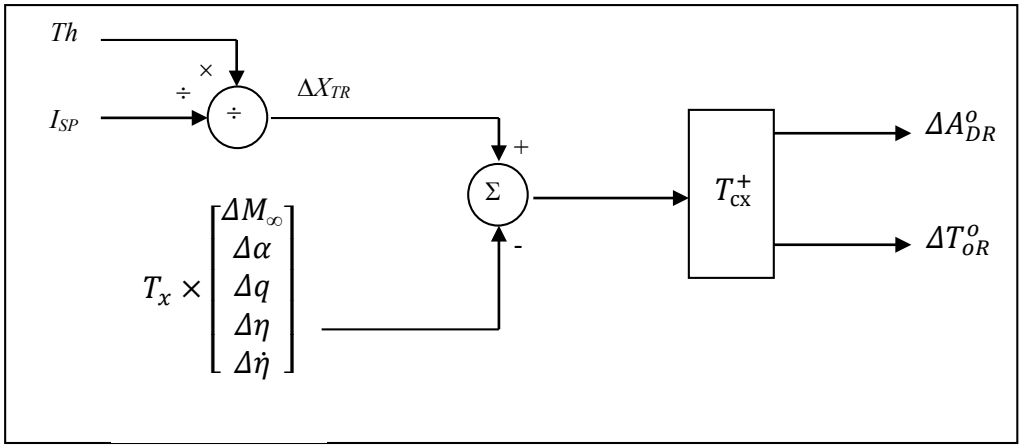

Fig. 14 Obtaining ΔX_T, A_{DR}^o and T_{oR}^o. (Note the pseudoinverse of T_{cx})

$\Delta\delta_F^o$ was not used directly in the engine dynamics analysis. $\Delta\delta_F^o$, ΔA_{DR}^o and ΔT_{oR}^o were feedback variables to the aircraft dynamics via the matrix, B. If $\Delta A_{DR}^o \approx \Delta A_D^o$ and $\Delta T_{oR}^o \approx \Delta T_o^o$, then the controlled aircraft with the proposed engine dynamics should remain stable.

VII. RESULTS FROM THE SIMULATION

With the Simulink model in place, the aircraft closed-loop system, subjected to the same 1000 ft commanded altitude change, was simulated. Under these conditions, the controlled aircraft with the new engine dynamics became unstable. Upon investigation, the cause of the instability was identified as the engine dynamics time constant. Initially, the time constant had been set to 0.5 s for this part of the experiment. However, 0.5 s proved to be too long for the optimal controls to react and stabilize the aircraft. The engine time constant was therefore reduced to 0.01 s, and the simulation was repeated, yielding stable responses. It was determined that the maximum time constant Hyperion could tolerate while maintaining stability was 0.07 s. Any value greater than this resulted in instability of the closed-loop system. The stable responses obtained with the new engine time constant are shown in Fig. 15 and Fig. 16.

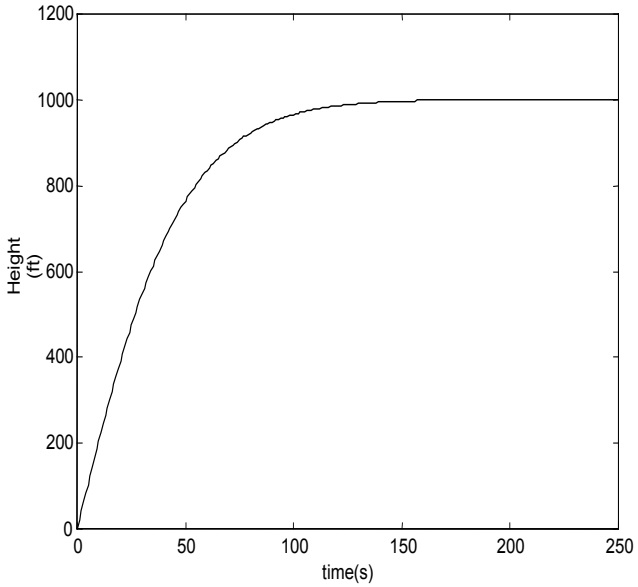

Fig. 15 The height response of Hyperion with the proposed engine dynamics

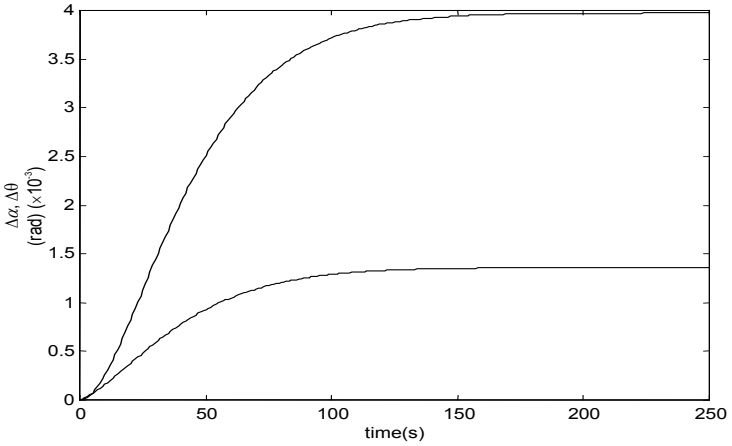

Fig. 16 Aircraft Closed-Loop Responses To A Commanded Change In Height With Engine Dynamics Included.

From the simulation, it was observed that as a consequence of including the engine dynamics in the aircraft dynamics, the values of the state variables of the aircraft were not identical to those obtained without engine dynamics. This suggests that including the engine dynamics in the aircraft also changed its dynamics. However, the changes were very small and did not persist.

Another interesting set of results obtained was the differences between the optimal controls before entering the engine dynamics and after exiting the engine dynamics. Since $\Delta\delta_F^o$ was not involved in the engine dynamics work, the change in this control variable was identical for both cases (See Fig. 17).

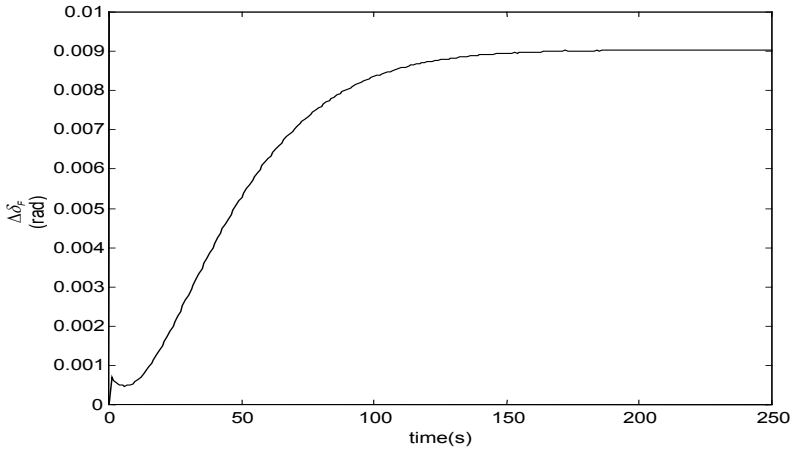

Fig. 17 The flaps (δ_F) response when aircraft is subjected to a commanded input.

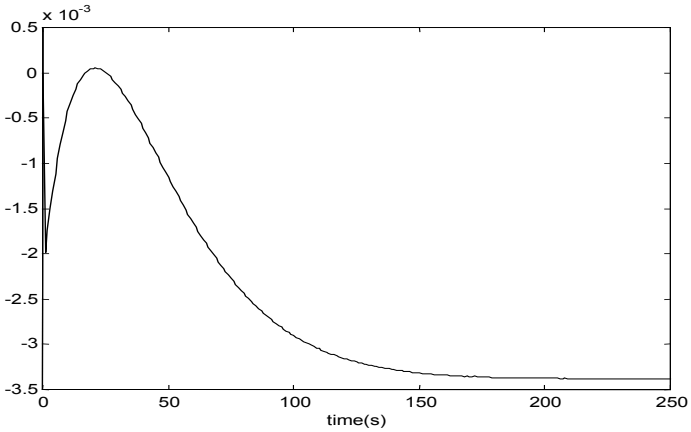

Fig. 18 The diffuser (A_D) response when aircraft is subjected to a commanded input.

The flaps on Hyperion reached a steady-state value of 0.009 rad after 180 seconds. ΔA_D^o appeared to be unaffected also by the inclusion of the engine dynamics. The response of this control to the commanded change is shown in Fig. 18.

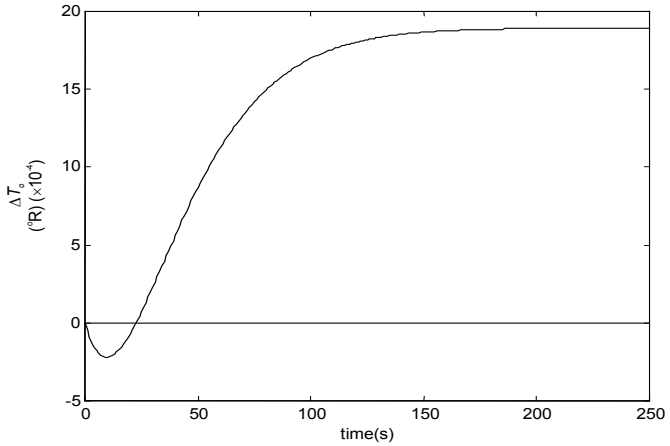

Fig. 19 ΔT_o^o and ΔT_{oR}^o

However, the response of ΔT_o^o and ΔT_{oR}^o were not the same and are presented in Fig. 19. The difference in the reconstructed ΔT_o control did not cause the aircraft to lose stability. This suggested that this control had little effect on the aircraft stability, and here it was confirmed that such a persistent difference as shown in Fig. 19 had no effect on the stability of the aircraft. The responses of ΔX_T and the thrust will be analysed next. The perturbation in the thrust force, ΔX_T, and the response of the engine thrust for Hyperion with the engine dynamics are shown in Fig. 20 and Fig. 21 respectively.

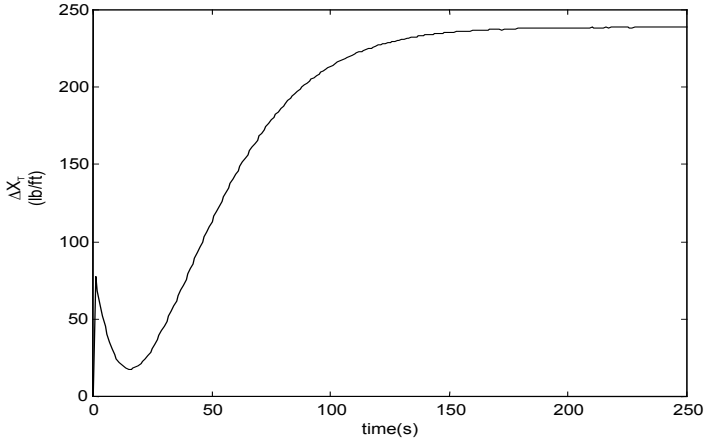

Fig. 20 The perturbation in the thrust force, ΔX_T.

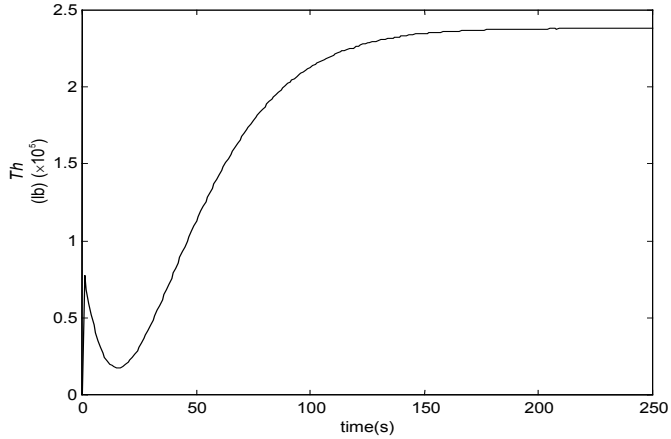

Fig. 21 Thrust Response

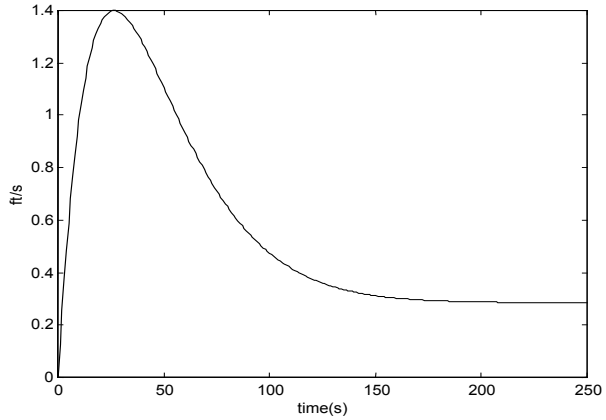

Fig. 22 Aircraft speed response

The response of ΔX_T peaked sharply at 77.7 lb/ft at 1 s but quickly decreased, reaching a minimum of 17.6 lb/ft at 16 s. The response then gradually increased and settled at a steady-state value of 238 lb/ft after 180 s. The thrust response exhibited a similar trend to ΔX_T . Thrust peaked at 69,370 lb at 1 s, then immediately decreased to a minimum of 15,717 lb. Thereafter, the thrust response increased gradually and, after 180 s, reached a steady-state value of 2.3×10^5 lb. This permanent change in thrust indicates an increase from the original value at the specified flight condition (not available from the aircraft's mathematical model). Since the thrust response reached a steady-state, this suggests that the change in thrust is not continuous.

Fig. 22 shows that the aircraft speed response reached a steady-state value of 0.284 ft/s; hence, no forward acceleration exists once steady-state is achieved. At this stage, it is difficult to assess whether the thrust magnitude is reasonable without comparable results. Similarly, it remains uncertain whether ΔX_T is appropriate for use as a fuel flow rate command for the proposed engine dynamics. However, the responses of the state variables, ΔX_T and *Th*, appeared consistent, i.e., an increase in ΔX_T caused an increase in *Th*.

VIII. CONCLUSION

A mathematical model of engine dynamics for a hypersonic vehicle was tested using the simulation software package Simulink and was found to produce results consistent with the formulations presented in [5] and [6]. The outputs included fuel equivalence ratio, specific impulse, and net thrust. This engine dynamics model was incorporated into the Hyperion closed-loop dynamics. Data on fuel flow rate were not directly available from Hyperion. Instead, the perturbation in thrust force along the x-axis (ΔX_T) was used as the fuel flow rate input to the mathematical model. Hyperion, with the integrated engine dynamics model, was simulated for flight at Mach 8.0 and an altitude of 100,000 ft. The aircraft control system was configured to produce a specified set of closed-loop eigenvalues. Dynamic stability was achieved, provided the engine time constant did not exceed 0.07 seconds. The closed-loop dynamics of Hyperion changed slightly due to the inclusion of the engine dynamics; however, the change was negligible, and the Stability Augmentation System (S.A.S.) maintained closed-loop stability. The S.A.S. design was based on Linear Quadratic Regulator (LQR) theory.

Declaration of Conflicting Interests
The authors declare no potential conflicts of interest with respect to the research, authorship, and/or publication of this article.

Funding
The authors received no financial support for the research, authorship, and/or publication of this article.

Use of Artificial Intelligence (AI)-Assisted Technology for Manuscript Preparation
The authors confirm that no AI-assisted technologies were used in the preparation or writing of the manuscript, and no images were altered using AI.

REFERENCES

[1] F. R. Chavez and D. K. Schmidt, "Analytical aeropropulsive/aeroelastic hypersonic-vehicle model with dynamic analysis," *J. Guid. Control Dyn.*, vol. 17, no. 6, pp. 1308-1319, 1994, doi: 10.2514/3.21349.

[2] D. K. Schmidt and J. Velapoldi, "Flight dynamics and feedback guidance issues for hypersonic airbreathing vehicles," in *Proc. AIAA Guid., Navig., Control Conf. Exhibit.*, Portland, OR, USA, 1999, Paper AIAA-1999-4122, doi: 10.2514/6.1999-4122.

[3] D. McLean and Z. A. Zaludin, "Stabilization of longitudinal motion of a hypersonic transport aircraft," *Trans. Inst. Meas. Control*, vol. 21, no. 2-3, pp. 99-105, 1999, doi: 10.1177/014233129902100206.

[4] Z. A. Zaludin, "Regaining loss in dynamic stability after control surface failure for an air-breathing hypersonic aircraft flying at Mach 8.0," *Asian Rev. Mech. Eng.*, vol. 10, no. 2, pp. 1-9, 2021, doi: 10.51983/arme-2021.10.1.2961.

[5] D. L. Raney, M. R. Phillips, and L. H. Person, "Investigation of piloting aids for manual control of hypersonic maneuvers," NASA, VA, USA, Tech. Rep. NASA TP-3525, 1995. [Online]. Available: https://ntrs.nasa.gov/citations/19960002013

[6] D. L. Raney and F. J. Lallman, "Control integration concept for hypersonic cruise-turn maneuvers," NASA, VA, USA, Tech. Rep. NASA TP-3136, 1992. [Online]. Available: https://ntrs.nasa.gov/citations/19920010953

[7] Z. A. Zaludin, "Mathematical model of an aircraft flying over a range of hypersonic speeds and heights," Aeronautics and Astronautics Department, Southampton Univ., Southampton, U.K., Tech. Rep. AASU 98/01, 1998.